AJNR

This information is current as of May 18, 2025.

Flat Panel Detector Angiographic CT for Stent-Assisted Coil Embolization of Broad-Based Cerebral Aneurysms

G. Richter, T. Engelhorn, T. Struffert, M. Doelken, O. Ganslandt, J. Hornegger, W.A. Kalender and A. Doerfler

ORIGINAL RESEARCH

G. Richter
T. Engelhorn
T. Struffert
M. Doelken
O. Ganslandt
J. Hornegger
W.A. Kalender
A. Doerfler

Flat Panel Detector Angiographic CT for Stent-Assisted Coil Embolization of Broad-Based Cerebral Aneurysms

BACKGROUND AND PURPOSE: The purpose of this work was to evaluate angiographic CT (ACT) in the combined application of a self-expanding neurovascular stent and detachable platinum coils in the management of broad-based and fusiform intracranial aneurysms.

MATERIALS AND METHODS: Eleven patients harboring wide-necked intracranial aneurysms were treated with a flexible self-expanding neurovascular stent and subsequent aneurysm embolization with platinum microcoils. ACT was performed after the interventional procedure to analyze stent position and the relationship of coils to the stent. Postprocessing included multiplanar reconstructions (MPRs) and maximum intensity projections (MIPs). ACT volume datasets were postprocessed for soft tissue visualization.

RESULTS: Accurate stent placement with subsequent coil occlusion of the aneurysms was feasible in all of the patients. Similar to nonsubtracted digital subtraction angiography (DSA) images, radiopaque platinum stent markers showed excellent visibility in ACT as well. The stent struts themselves, hardly visible in nonsubtracted DSA, were visible in MPRs and MIPs of ACT in all of the patients. In aneurysms larger than 10 mm in diameter, accurate stent assessment at the level of the coils was limited due to beam hardening artifacts. Postprocedural ACT in all of the patients did not reveal any evidence of procedure-related intracranial hemorrhage.

CONCLUSION: ACT provides cross-sectional, 3D visualization of endovascular stents otherwise hardly visible with plain fluoroscopy. ACT enables us to accurately determine stent position, which may be helpful in complex stent-assisted aneurysm coiling procedures. However, in aneurysms larger than 10 mm in diameter, beam hardening artifacts caused by the endoaneurysmal coil package impair visibility of the stent. Further data are necessary to evaluate the usefulness of ACT in stent-assisted aneurysm coiling.

The International Subarachnoid Aneurysm Trial[1] showed intracranial aneurysms treatable with either neurosurgical clipping or endovascular coiling to be better treated with endovascular coiling because of a significantly more beneficial clinical outcome compared with neurosurgical aneurysm clipping. The unfavorable geometry of wide-necked aneurysms is associated with a significant risk of coil prolapse in the parent artery. One therapeutic option is the balloon-assisted aneurysm remodeling technique first described in 1997 by Moret et al.[2] Feasibility of this technique is proved[3]; however, it may be correlated with an increased incidence of complications.[4]

Another therapeutic solution for wide-necked aneurysms is using a scaffold to bridge the aneurysm neck with subsequent coiling through the stent interstices. The currently available, highly flexible self-expanding microstents enable treatment of wide-necked aneurysms.[5] Meanwhile, stent-assisted aneurysm coiling is well established in clinical routine.[5-9] However, fluoroscopic and plain radiographic visibility of the stent struts is especially limited by the low profile of these highly flexible devices,[10] with only the proximal and distal radiopaque stent markers visible. This may render it difficult

to exactly assess stent position and adaptation of stent struts to the vessel wall.[11]

Angiographic CT (ACT) uses rotational, C-arm mounted flat panel detector technology capable of high spatial resolution volumetric imaging.[12] Using this ACT imaging may enable adequate visualization of stent position and especially the stent struts.[10,11] This technique may improve procedural safety and efficacy of stent-assisted aneurysm coiling and it may enhance our understanding of intracranial stent deployment. In addition, ACT image quality seems to be sufficient in the detection of neuroendovascular procedural complications.[13]

The aim of our study was to evaluate ACT in the combined application of a self-expanding neurovascular stent and detachable platinum coils in the management of broad-based and fusiform intracranial aneurysms.

Materials and Methods

Patients

From April to November 2006, 11 consecutive patients harboring a wide-necked or fusiform intracranial aneurysm were treated with a Neuroform microdelivery stent system (Neuroform Microstent System; Boston Scientific Corp, Fremont, Calif) and subsequent aneurysm embolization using detachable platinum coils (Table 1). Selection criteria included a wide-necked or fusiform aneurysm assumed untreatable with coil packing only. A wide neck was defined as neck diameter more than 5 mm or an unfavorable head-to-neck ratio less than 1.5, confirmed by digital subtraction angiography (DSA). Aneurysm diameter ranged from 2.5 to 18 mm, with a mean diameter of 9.1 mm.

Table 1: Characteristics of patients treated with stent-assisted coiling

Case-No. (Age, y)	Sex	Aneurysm Localization	Presenting Symptoms	Maximum Aneurysm Diameter, mm	Maximum Aneurysm Neck Diameter, mm	Head/Neck Ratio
1 (66)	F	ICA, extradural	Progressive, ipsilateral visual impairment	18	6	3.0
2 (63)	M	Basilar stem	Asymptomatic, elective procedure	4	3.5	1.1
3 (35)	M	Basilar stem	SAH Hunt and Hess grade 4	4.5	3.5	1.3
4 (61)	F	Basilar tip	Brain stem compression, hydrocephalus	13	7	1.3
5 (57)	M	Basilar tip	SAH Hunt and Hess grade 4 at time of previous coiling	12	5.5	2.2
6 (24)	F	ICA Multilobulated	No symptoms, elective procedure	10	6	1.7
7 (44)	M	Basilar stem	SAH Hunt and Hess grade 3 at time of previous coiling	2.5	2	1.25
8 (45)	F	Basilar tip	SAH Hunt and Hess grade 3	10	5.5	1.8
9 (46)	F	Basilar tip	SAH Hunt and Hess grade 1	11	6	1.8
10 (58)	M	Fusiform vertebral artery aneurysm with saccular comp	Asymptomatic, previous SAH from inversely located vertebral aneurysm	4 (saccular compartment)	No neck, fusiform geometry	–
11 (47)	M	Fusiform vertebral artery aneurysm	Asymptomatic	11	No neck, fusiform geometry	–

Note:—ICA indicates internal carotid artery; M, male; F, female; SAH, subarachnoid hemorrhage; –, no data.

Table 2: Results and cases arbitrarily divided into 3 groups in terms of stent visibility with angiographic CT data reconstructions*

Case No. (Age, y)	Stent (Neuroform 2/3)	Maximum Aneurysm Diameter, mm	No. of coils	Aneurysm Occlusion Rate, I > 95% or II < 95%	Stent Visibility, Grade 1, 2, or 3
1 (66)	NF3, 4.5 × 20 mm	18	18	II	3
2 (63)	NF3, 4.5 × 20 mm	4	2	II	1
3 (35)	NF3, 4.5 × 20 mm	4.5	5	I	1
4 (61)	NF3, 4.0 × 20 mm	13	4	II	3
5 (57)	NF3, 4.0 × 20 mm	12	7	I	2
6 (24)	NF2, 4.5 × 20 mm	10	10	I	2
7 (44)	NF3, 4.0 × 20 mm	2.5	3	I	1
8 (45)	NF3, 3.5 × 20 mm	10	8	I	2
9 (46)	NF3, 4.0 × 20 mm	11	14	II	3
10 (58)	NF3, 4.0 × 20 mm	4 (saccular compartment)	7	I	3
11(47)	NF3, 4.5 × 30 mm	11	11	I	3

Note:—NF indicates Neuroform.
* Group 1, excellent; Group 2, favorable; Group 3, poor (see column on the right).

Feasibility of stent deployment at the desired place, as well as aneurysm occlusion rate, was documented. Hereby, we classified 2 groups of angiographic findings. First, complete or nearly complete (>95%) occlusion included no residual aneurysm, minimal small dog ear remnant, or area of concavity at the level of the aneurysm neck. Second, subtotal (<95%) occlusion included a clearly visible residual neck and/or remarkable filling within the interstices of the coils either at the neck and/or at the body of the aneurysm. Retreatment in this group is always considered.

Aneurysms were located at the internal carotid artery ($n = 2$), basilar tip encroaching at least 1 P1 segment ($n = 4$), basilar stem ($n = 3$), and intracranial vertebral artery ($n = 2$). Five ($n = 5$ of 11) aneurysms were ruptured; 3 of them were treated with stent-assisted coil embolization initially. Two of the ruptured aneurysms were initially treated with coil embolization only, presenting with a subsequent coil compaction and partial aneurysm reperfusion during follow-up. Six ($n = 6$ of 11) aneurysms were unruptured; 4 of them were asymptomatic. Two patients harbored giant aneurysms with local compression symptoms (Table 1), and 1 had an extradural giant aneurysm of the internal carotid artery with increasing visual impairment due to optic nerve compression. The other patient had a partially thrombosed giant aneurysm of the basilar tip with consecutive occlusive hydrocephalus and progredient, symptomatic brain stem compression.

All of the patients with unruptured aneurysms ($n = 6$) were premedicated with double antiplatelet therapy consisting of aspirin (100 mg) and a loading dose of clopidogrel (300 mg) orally given the day before the procedure. In all of the patients, clopidogrel (75 mg per day) was continued for an additional 6 weeks, and aspirin (100 mg per day) for lifetime. All of the patients received heparin to raise the activated clotting time to 300 seconds during the procedure and for the following 48 hours. The patients with acute subarachnoid hemorrhage (SAH) received clopidogrel (loading dose of 300 mg) via gastric tube and aspirin (500 mg) intravenously immediately before stent placement. Stent-assisted aneurysm coiling procedure was performed under general anesthesia in all of the subjects.

Intracranial Self-expandable Stent and Coils
The latest generation of intracranial, self-expandable open-cell design stents (Neuroform 2 and Neuroform 3 microdelivery stent systems; Boston Scientific Corp) used in this series has a low stent profile and is highly flexible, respectively. The stent has 4 proximal and distal radiopaque markers, respectively. The stent itself is hardly visible with current standard techniques, such as digital radiography, fluoroscopy, or standard CT. Stent placement was performed over a 0.0014-inch exchange wire (Transend Floppy; Boston Scientific Corp). For subsequent aneurysm embolization, 2D and complex-shaped

(Guglielmi detachable coil [GDC] 360°) bare coils (Boston Scientific Corp) were used. GDC-18 and GDC-10 were used in the 4 subjects with aneurysm diameters larger than 10 mm and GDC-10 exclusively in the remaining 7 aneurysms.

ACT Imaging

ACT was performed after stent release in 3 cases and after stent release and subsequent coil insertion in all of the 11 cases. Data acquisition was performed with a biplane, flat panel detector angiography system (Axiom Artis dBA; Siemens Medical Solutions, Forchheim, Germany) and commercially available software (DynaCT; Siemens Medical Solutions), whereas postprocessing was performed with a separate workstation (Leonardo; Siemens Medical Solutions). ACT data acquisition was performed using the following parameters: acquisition time, 20 seconds; 1240×960 projection matrix; projection on 30×40 cm flat panel size; 217° rotation angle; 543 images in total; and increment 0.4° per image. The standard system dose is 0.36×10^{-6} Gy per image resulting in a total dose of 22 mGy per ACT acquisition. Acquisition of ACT volume data for stent and coil assessment was performed without contrast agent administration.

Postprocessing consisted of computed correction of beam hardening, ring artifacts, and scattered radiation (DynaCT-preset). The selectable postprocessing algorithm included setting "bone-kernel" and "hard" image characteristics. Secondary calculations of image data were performed with a volume of approximately $7.5 \times 7.5 \times 7.5$ cm, 512×512 matrix, with a resulting isotropic voxel size of approximately 0.15 mm in each plane. MPRs and MIPs were used for visualization of inserted stents and platinum coils. MPRs in axial and sagittal orientation to the stent were obtained for better visualization of stent patency or potential prolapse of stent struts in the aneurysm base. Additional MIPs were calculated to provide an overview of stent and coil package.

Other than conventional DSA imaging, rotational, 3D angiography with automatic contrast agent injection (from 1.5 up to 2.5 mL/s dependent on catheter position and vascular territory) before and after the intervention was performed in each case, using a program with a single rotation time of 5 seconds (total contrast agent injection time, 6.5 seconds, 1.5 seconds delay) after a 5-second native mask acquisition run.

Two experienced neuroradiologists together assessed the ACT reconstructions and divided the cases arbitrarily into 3 groups in terms of stent visibility (group 1 = excellent; group 2 = favorable; group 3 = poor). Intention was to achieve conjoined agreement. The continuously visible stents (including the stent struts between the radiopaque distal markers, especially these that are on the same level with the coil package) were allocated in group 1. Group 2 covered the cases with limited visibility of the stent struts adjacent to the coil package. It was impossible to accurately depict the stent segment facing the coil package exclusively. Group 3 included the cases in which the whole stent proved to be virtually invisible, except the terminal radiopaque markers.

Follow-up DSA was recommended for all of the patients and was performed 6 months after intervention. If baseline DSA and MR angiography (MRA) and the examination after 6 months reveals identical results, further follow-up was usually done by MRA alone.

Results

Technical Results and Complications

Stent-assisted coil embolization was feasible in all of the aneurysms ($n = 11$). Aneurysm occlusion was classified as complete in 7 and subtotal in 4 cases, respectively. In all of the patients, stent deployment was safely achieved at the desired location in the initial attempt. Stent placement prevented coil herniation into the parent artery in all of the cases.

One patient developed space-occupying bleeding in the right cerebral hemisphere 2 days after the stent-assisted aneurysm coiling of the fusiform vertebral artery aneurysm. He showed neurologic deterioration with hemiataxia with a good recovery after 30 days. There was neither in-stent thrombosis nor aneurysm wall perforation during the procedure.

ACT Imaging Findings

MPR in axial and sagittal orientation to the stent with 1.5-mm-section thickness confirmed that there was no case with recognizable prolapse of stent struts into the aneurysm base. ACT did not demonstrate any case of coil dislocation into the parent vessel or in between the stent and parent artery wall.

Two experienced neuroradiologists divided the ACT reconstructions performed after aneurysm coiling into 3 groups in terms of stent visibility (group 1 = excellent; group 2 = favorable; group 3 = poor). Conjoined agreement was achieved in all of the cases (Table 2).

Stent visibility was best in the 3 cases in which we performed ACT after stent deployment and before coil insertion. Three of 4 cases treated with platinum coils up to 5 mm in diameter showed excellent stent visibility ($n = 3$ of 11; stent visibility group 1), 1 case (case 10) with a fusiform vertebral aneurysm where the coils enclosed the stent circularly on a distance of approximately 1.5 cm revealed poor stent visibility (stent visibility group 3).

Two stents used for the aneurysms treated with coils up to 10 mm in maximum diameter ($n = 2$ of 11) revealed favorable visibility (stent visibility group 2). The 5 stents used for aneurysms larger than 10 mm in diameter showed favorable (group 2; $n = 1$ of 11) or dissatisfying (group 3; $n = 4$ of 11) visibility in the ACT reconstructions, respectively. The 3 cases with excellent visibility of the inserted stent allowed definite exclusion of coil prolapse through the stent interstices in the axial MPR reconstructions due to minimal beam hardening artifacts only. In the 3 cases with favorable stent visibility, the assessment of potential coil prolapse or herniated stent struts was not possible in the contact area between coil package and stent wall only. Adjacent stent regions showed good visibility.

In the 5 cases allocated to stent visibility group 3, the Neuroform stent section distant to the coil package was visible only. Potential coil prolapse, thus, could have remained unnoticed. Beam hardening artifacts from adjacent skull bone, especially in the basilar artery cases, were existent but turned out to have no significant influence on stent assessment with ACT.

Two cases with SAH Hunt and Hess grades 3 and 4, respectively, which showed hyperattenuated blood in the ACT imaging, had changeless findings in pre- and postprocedural ACT imaging. The remaining cases where, without detectable hyperattenuated lesions or mass effect after stent-assisted aneurysm coiling, were confirmed by postprocedural CT and MR imaging. It was possible to assess the CSF spaces, especially with regard to potential hydrocephalus in SAH treatment in all of the 11 cases. Postprocedural ACT performed within the angio suite revealed no evidence of procedure-related intra-

Fig 1. *A,* The basilar stem aneurysm showed complete occlusion initially after insertion of a single coil 2.5 mm in diameter: coil compaction and significant aneurysm growth in 6-month follow-up-DSA. *B,* Unsubtracted DSA image after insertion of a Neuroform stent (4 × 20 mm) shows the proximal and distal radiopaque markers of the stent (*arrows*); the stent itself is not visible. *C,* MIP reconstruction of ACT performed after stent deployment and before second coil embolization: excellent stent visibility and regular, complete stent deployment. The initially inserted single coil shows compaction and is distant to the parent (basilar) artery and to the stent struts as well, including one coil loop with position adjacent to stent wall, with definite extraluminal position. *D,* DSA. A total of 4 platinum microcoils (diameters, 2.5 and 2.0 mm, respectively) were additionally inserted. The basilar stem aneurysm shows satisfiable occlusion with minimal dog-ear remnant. *E,* Axial, thin (1 mm section thickness) MPR reconstruction of ACT performed after stent deployment and second coil embolization (same dataset as in *F*). This reconstruction allows definite exclusion of stent strut movement or coil protrusion: stent (*thin arrows*) without deformation adjacent to coil package (*thick arrow*), which causes some beam-hardening artifacts. *F,* MIP reconstruction (oblique coronal) of ACT performed after stent deployment and second coil embolization: excellent stent visibility without significant limitation by marginal beam-hardening artifacts through coil package; no change of stent configuration compared with the ACT imaging before the second coil embolization.

cranial hemorrhage in all of the cases confirmed by early MR imaging within 3 days after intervention.

Representative Cases

Case 7. Patient initially presented with SAH Hunt and Hess grade 3. DSA revealed a small basilar artery stem aneurysm, 2 mm in diameter, with signified aneurysm neck. A single coil (2 mm in diameter) was inserted with complete aneurysm occlusion initially. Six-month follow-up showed coil compaction and significant growth of the now broad-based aneurysm (Fig 1*A*). Stent-assisted aneurysm recoiling with a Neuroform 3 stent (4 × 20 mm) was recommended (Fig. 1*B*). ACT showed proper stent deployment in the MIP (Fig 1*C*). Recoiling included 3 platinum coils. Final DSA revealed sufficient aneurysm occlusion with minimal "dog-ear remnant" (Fig 1*D*). Finally, ACT showed unchanged stent configuration and no coil protrusion (Fig 1*E*, stent, *long arrows*; coil package, *thick arrow*) in the MIP similarly (Fig 1*F*).

Case 3. Patient presented with distinctive SAH Hunt and Hess grade 4. Blood clots were visible in the lateral ventricles in

the axial ACT reconstruction (Fig 2*A*). The DSA revealed a basilar artery stem aneurysm, 4.5 mm in diameter (3D DSA; Fig 2*B*). There was no adequate aneurysm neck for simple aneurysm coiling. After the stent-assisted coiling procedure, a small distal aneurysm remnant had to be accepted, because it proved impossible to insert a further coil inside the aneurysm sac (Fig 2*D*, *E*). Coiling procedure was followed by ACT, which showed regular stent deployment and exclusive endo-aneurysmal coil placement (Fig 2*F*).

Case 5. The patient suffered from SAH Hunt and Hess grade 4 initially. DSA showed a large aneurysm of the basilar tip, 12 mm in diameter, and 2 nearly inversely configured aneurysms in the angles between the posterior cerebral artery and superior cerebellar artery origins, 2.5 and 2 mm in diameter, respectively. Hemorrhage was regarded to originate from the large basilar tip aneurysm. Coiling of the basilar tip aneurysm was performed in standard technique. Follow-up DSA was performed 3 months later, and the basilar tip aneurysm showed reperfusion due to coil compaction and aneurysm growth, and the adjacent 2 basilar aneurysms were unchanged
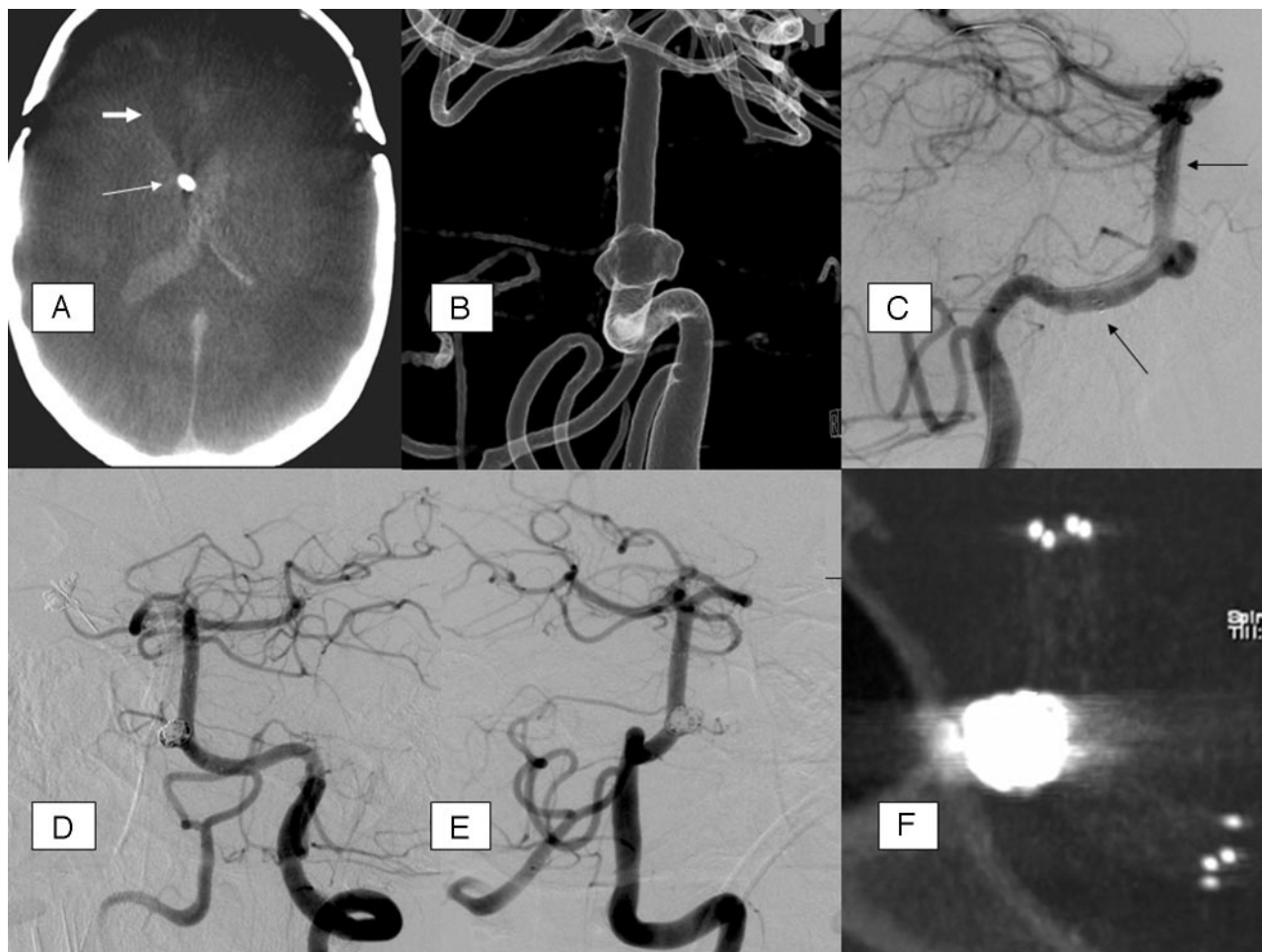
Fig 2. *A*, Native, axial ACT-reconstruction, 5 mm section thickness; extensive SAH with intraventricular, hyperattenuated blood; CSF drainage adjacent to the septum pellucidum (*arrow*); previous frontal trepanation in the course of aneurysm clipping (anterior communicating artery); hypoattenuated brain parenchyma defect (*thick arrow*) with dilation of the frontal of the right lateral ventricle due to previous aneurysm rupture and parenchymal hemorrhage. *B*, Rotational 3D angiography with intra-arterial contrast agent injection, transparent surface shaded reconstruction (posterior-anterior view); broad-based proximal basilar stem aneurysm, forward oriented. The aneurysm base surrounds the basilar artery at least as a semicircle. *C*, DSA, lateral view; guidewire in the left posterior cerebral artery; Neuroform stent with proximal and distal markers (*arrows*). *D* and *E*, DSA (oblique views) after stent-assisted aneurysm coiling. *F*, MIP reconstruction of ACT after stent-assisted aneurysm coiling, providing excellent overview of the stent and the adjacent coil package; moderate beam-hardening artifacts.

(Fig 3*A*). A 4 × 20 mm Neuroform 3 stent was placed across the broad-based aneurysm neck (Fig 3*B*, microguidewire; Fig 3*C*, Neuroform stent in position, still undeployed with radiopaque markers, *arrows*; note: basilar artery/posterior cerebral artery passage is stretched significantly). Subsequent coiling of the basilar tip aneurysm (Fig 3*D*), the aneurysm of the posterior cerebral artery/superior cerebellar artery (SUCA) angles, was not attempted for coil occlusion because the outlet of the SUCA arises out of the small aneurysms on both sides. ACT showed good visibility of the basilar section of the stent, though the stent segment in the posterior cerebral artery was significantly impaired by beam-hardening artifacts of the coil package (Fig 3*E*). ACT revealed no bleeding with mass effect (Fig 3*F*, proximal stent markers with *white arrow*).

Discussion

For patients undergoing stent-assisted coil embolization of broad-based aneurysms, early recognition of procedure-related complications may be essential, such as incomplete stent deployment, stent migration, or coil dislocation during the procedure or intracranial hemorrhage due to perforation of the aneurysm or the parent artery. Currently the commercially

available intracranial self-expandable stents are hardly visible in fluoroscopy; only the terminal radiopaque markers of the Neuroform stent provide gross overview of the stent position. However, exact position, especially of the stent struts at the aneurysm neck, remains unclear. Even incomplete stent deployment or deficient fitting of the stent to the vessel wall may remain unnoticed. This deficit may play a role in complex aneurysms or curved vessel anatomy, especially, for instance, in cases with significant changing of parent vessel diameter and bifurcations.[10]

The use of ACT in cerebrovascular stent placement was described previously for balloon-mounted intracranial deployed stents[11] and for a single Neuroform stent,[10] respectively. ACT provides high-quality imaging of Neuroform stents; even the strut network of the stents is visible in 3D MIP and MPR.[11]

The purpose of our study was to evaluate ACT in stent-assisted coil embolization of broad-based and fusiform intracranial aneurysms. MPR in axial and sagittal orientation to the stent and MIP of the stent obtained excellent images in the 3 cases of this small series with ACT performed after stent deployment and before the coiling procedure.
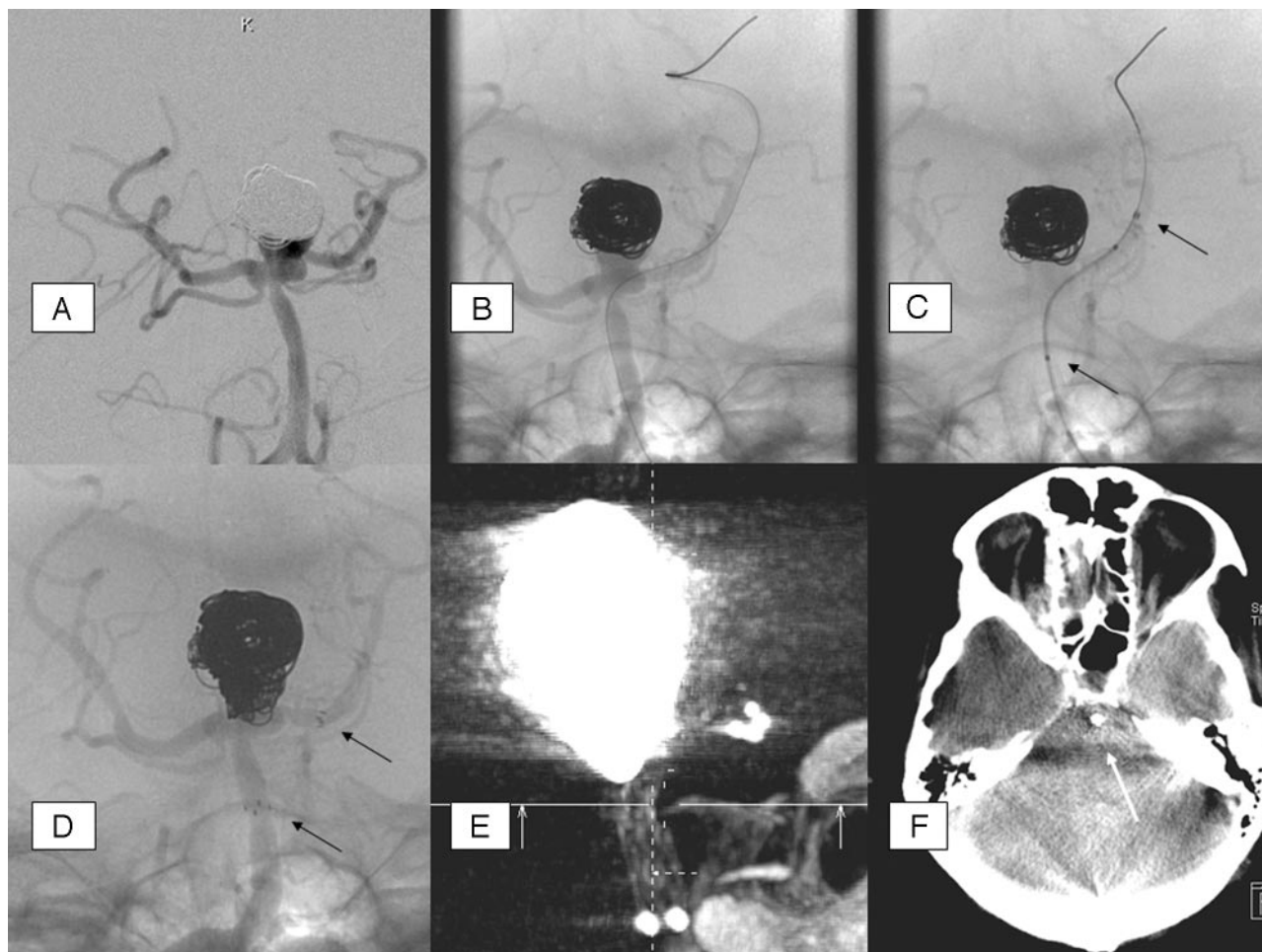
Fig 3. *A*, Follow-up DSA 3 months after initial coiling of the basilar artery tip aneurysm; partially reperfused aneurysm due to aneurysm growth and minimal coil compaction. *B*, Exchange microguidewire in the left posterior cerebral artery. *C*, Neuroform stent inserted, still undeployed, with radiopaque markers at the ends (*arrows*). Note the stretched vessel anatomy compared with *B. D*, Fully deployed stent, markers (*arrows*). *E*, ACT MIP reconstruction with impaired stent visibility on the level of the large coil package. *F*, ACT with MPR to exclude periprocedural bleeding; proximal stent marker (*arrow*).

Excellent or at least favorable overview of the stent with the adjacent coil package was achieved in the cases with coil package diameter up to 10 mm. ACT volume data MIP and MPR performed in our cases with aneurysm (coil package) size smaller than 10 mm allowed exclusion of coil prolapse through the stent struts, even when beam-hardening artifacts were distinctive. ACT findings in cases with coil packages larger than 10 mm in diameter were not adequate to assess the interesting stent portion adjacent to the coil package due to beam-hardening artifacts. The ACT data of these latter cases allowed evaluation of the stent portions not adjacent to the coils only.

The extent of the beam-hardening artifacts seems to depend on the "coil package size" and "coil packing attenuation," both determining the radiopacity of the coil package in the course of the x-ray beam. The occurrence of these artifacts correlates with the coil package diameter at least in this small series, though the coil packing attenuation was different in some limits of variation.

Thus, ACT imaging seems to be an excellent tool for stent visualization in cases with aneurysms up to 10 mm in diameter, whereas the stent visualization in cases with larger aneurysms is significantly impaired by beam-hardening artifacts.

Further ACT imaging may be helpful, especially in cases with fusiform aneurysm geometry or at least a semicircle coil package around the stent, when concise fluoroscopy projection is impossible.

These findings are in line with the study results of Trossbach et al,[14] who evaluated intracranial small vessel stents used for angioplasty with conventional CT angiography, which proved to be considerably impaired by beam-hardening artifacts. As a result of this study, ACT imaging seems to be impaired by beam-hardening artifacts to a lesser extent; it is actually possible to assess intracranial, low-profile stents adjacent to coil packages smaller than 10 mm in diameter.

Windowing of the ACT image data was adapted individually, with an image aspect comparable with bone window in conventional CT imaging for the stent visualization. Obtainable optimum in stent visibility was achieved with window values displayed at approximately 1000 for window width (W) and 500 for window level (C). The image windowing used for morphologic ACT brain imaging showed optimal contrast solution at approximately 240 W and 80 C.

Periprocedural aneurysm rupture as a potential, serious complication seems to be especially detectable with ACT, as reported in particular cases.[13] These morphologic, CT-like

ACT images may allow exclusion of gross intracranial hemorrhage, a feature with presumably high clinical relevance in complication management. There was no case with gross periprocedural hemorrhage in our small series. It was possible to assess the CSF spaces especially with regard to potential hydrocephalus in SAH treatment in all of the 11 cases.

ACT acquisition in the course of stent-assisted aneurysm coiling provides good overview of stent position and deployment with contrast and spatial resolution superior to fluoroscopy and unsubtracted DSA images in our series. This may be of special interest in cases with complex aneurysm geometry and perhaps especially in the stent-assisted treatment of fusiform aneurysms.

Comparison of radiographic appearance in baseline and follow-up examinations in 2 plain radiographic planes of coiled aneurysms was used to predict potential angiographic aneurysm instability. Change of radiographic appearance allowed prediction of angiographic aneurysm instability with an accuracy of 76%.[15] As a future perspective, ACT imaging may be exclusively of interest for noninvasive follow-up of aneurysms treated with stent-assisted coiling. It may possibly have potential to predict the stability of aneurysms treated with stent-assisted coiling in select individual patients for invasive control angiography.

Conclusion

ACT provides cross-sectional, 3D visualization of endovascular stents that are otherwise hardly visible with plain fluoroscopy. ACT enables accurate determination of stent position, which may be helpful in complex stent-assisted aneurysm coiling procedures. However, in aneurysms larger than 10 mm in diameter, beam-hardening artifacts caused by the endoaneurysmal coil-package impair visibility of the stent. Further data are necessary to evaluate the usefulness of ACT in stent-assisted aneurysm coiling.

References

1. Molyneux AJ, Kerr RS, Yu LM, et al. **International subarachnoid aneurysm trial (ISAT) of neurosurgical clipping versus endovascular coiling in 2143 patients with ruptured intracranial aneurysms: a randomised comparison of effects on survival, dependency, seizures, rebleeding, subgroups, and aneurysm occlusion.** *Lancet* 2005;366:809–17
2. Moret J, Cognard C, Weill A, et al. **Reconstruction technic in the treatment of wide-neck intracranial aneurysms. Long-term angiographic and clinical results apropos of 56 cases**. *J Neuroradiol* 1997;24:30–44
3. Baldi S, Mounayer C, Piotin M, et al. **Balloon-assisted coil placement in wide-neck bifurcation aneurysms by use of a new, compliant balloon microcatheter.** *AJNR Am J Neuroradiol* 2003;24:1222–25
4. Cottier JP, Pasco A, Gallas S, et al. **Utility of balloon-assisted Guglielmi detachable coiling in the treatment of 49 cerebral aneurysms: a retrospective, multicenter study.** *AJNR Am J Neuroradiol* 2001;22:345–51
5. Wanke I, Doerfler A, Schoch B, et al. **Treatment of wide-necked intracranial aneurysms with a self-expanding stent system: initial clinical experience.** *AJNR Am J Neuroradiol* 2003;24:1192–99
6. Howington JU, Hanel RA, Harrigan MR, et al. **The Neuroform stent, the first microcatheter-delivered stent for use in the intracranial circulation.** *Neurosurgery* 2004;54:2–5
7. Lee YJ, Kim DJ, Suh SH, et al. **Stent-assisted coil embolization of intracranial wide-necked aneurysms.** *Neuroradiology* 2005;47:680–89
8. Wanke I, Doerfler A, Goericke S, et al. **Treatment of wide-necked intracranial aneurysms with a self-expanding stent: mid-term results.** *Zentralbl Neurochir* 2005;66:163–69
9. Benitez RP, Silva MT, Klem J, et al. **Endovascular occlusion of wide-necked aneurysms with a new intracranial microstent (Neuroform) and detachable coils.** *Neurosurgery* 2004;54:1359–67
10. Benndorf G, Claus B, Strother CM, et al. **Increased cell opening and prolapse of struts of a Neuroform stent in curved vasculature: value of angiographic computed tomography: technical case report.** *Neurosurgery* 2006;58:ONS-E380
11. Benndorf G, Strother CM, Claus B, et al. **Angiographic CT in cerebrovascular stenting.** *AJNR Am J Neuroradiol* 2005;26:1813–18
12. Gupta R, Grasruck M, Suess C, et al. **Ultra-high resolution flat-panel volume CT: fundamental principles, design architecture, and system characterization.** *Eur Radiol* 2006;16:1191–205
13. Heran NS, Song JK, Namba K, et al. **The utility of DynaCT in neuroendovascular procedures.** *AJNR Am J Neuroradiol* 2006;27:330–32
14. Trossbach M, Hartmann M, Braun C, et al. **Small vessel stents for intracranial angioplasty: in vitro evaluation of in-stent stenoses using CT angiography.** *Neuroradiology* 2004;46:459–63
15. Connor SE, West RJ, Yates DA. **The ability of plain radiography to predict intracranial aneurysm occlusion instability during follow-up of endosacular treatment with Gugliemi detachable coils.** *Neuroradiology* 2001;43:680–86